Journal of Child Neurology
1-12

DOI: 10.1177/0883073820987742
journals.sagepub.com/home/jcn
SAGE

# Postmortem Analyses in a Patient With Succinic Semialdehyde Dehydrogenase Deficiency (SSADHD): II. Histological, Lipid, and Gene Expression Outcomes in Regional Brain Tissue

**Dana C. Walters[1], Regan Lawrence[2], Trevor Kirby[1], Jared T. Ahrendsen, MD, PhD[3], Matthew P. Anderson, MD, PhD[3], Jean-Baptiste Roullet, PhD[1], Eric J. Murphy, PhD[2], K. Michael Gibson, PhD[1]; and the SSADH Deficiency Investigators Consortium (SDIC)**

## Abstract

This study has extended previous metabolic measures in postmortem tissues (frontal and parietal lobes, pons, cerebellum, hippocampus, and cerebral cortex) obtained from a 37-year-old male patient with succinic semialdehyde dehydrogenase deficiency (SSADHD) who expired from SUDEP (sudden unexplained death in epilepsy). Histopathologic characterization of fixed cortex and hippocampus revealed mild to moderate astrogliosis, especially in white matter. Analysis of total phospholipid mass in all sections of the patient revealed a 61% increase in cortex and 51% decrease in hippocampus as compared to ($n = 2$-4) approximately age-matched controls. Examination of mass and molar composition of major phospholipid classes showed decreases in phospholipids enriched in myelin, such as phosphatidylserine, sphingomyelin, and ethanolamine plasmalogen. Evaluation of gene expression ($RT^2$ Profiler PCR Arrays, GABA, glutamate; Qiagen) revealed dysregulation in 14/15 $GABA_A$ receptor subunits in cerebellum, parietal, and frontal lobes with the most significant downregulation in $\varepsilon$, $\theta$, $\rho 1$, and $\rho 2$ subunits (7.7-9.9-fold). $GABA_B$ receptor subunits were largely unaffected, as were ionotropic glutamate receptors. The metabotropic glutamate receptor 6 was consistently downregulated (maximum 5.9-fold) as was the neurotransmitter transporter (GABA), member 13 (maximum 7.3-fold). For other genes, consistent dysregulation was seen for interleukin 1$\beta$ (maximum downregulation 9.9-fold) and synuclein $\alpha$ (maximal upregulation 6.5-fold). Our data provide unique insight into SSADHD brain function, confirming astrogliosis and lipid abnormalities previously observed in the null mouse model while highlighting long-term effects on GABAergic/glutamatergic gene expression in this disorder.

## Keywords

GABA, succinic semialdehyde dehydrogenase deficiency, GABA receptors, glutamate receptors, brain lipids, gene expression profiles

Received September 17, 2020. Received revised November 9, 2020. Accepted for publication December 19, 2020.

## Introduction

Succinic semialdehyde dehydrogenase (SSADH) deficiency (SSADHD) is an orphan heritable disorder of GABA metabolism (for pathway interrelationships; see figure 1 of the preceding article in this series, Kirby et al[1]). Patients with SSADHD manifest a nonspecific neurologic phenotype of global developmental delay, neuropsychiatric morbidity, absence of developed speech, and variable epilepsy.[2] Diagnosis based on clinical characteristics is unreliable but diagnosis can be obtained by metabolic analysis combined with molecular analysis of the ALDH5A1 gene (OMIM 610045; 271980;

[1] Department of Pharmacotherapy, College of Pharmacy and Pharmaceutical Sciences, Washington State University, Spokane, WA, USA
[2] Department of Biomedical Sciences, University of North Dakota School of Medicine and Health Sciences, Grand Forks, ND, USA
[3] Department of Pathology, Beth Israel Deaconess Medical Center and Harvard Medical School, Boston, MA, USA

**Corresponding Author:**
Mike Gibson, Department of Pharmacotherapy, College of Pharmacy and Pharmaceutical Sciences, Health Sciences Building Room 210C, Washington State University, 412 E. Spokane Falls Boulevard, Spokane, WA 99202-2131, USA.
Email: mike.gibson@wsu.edu

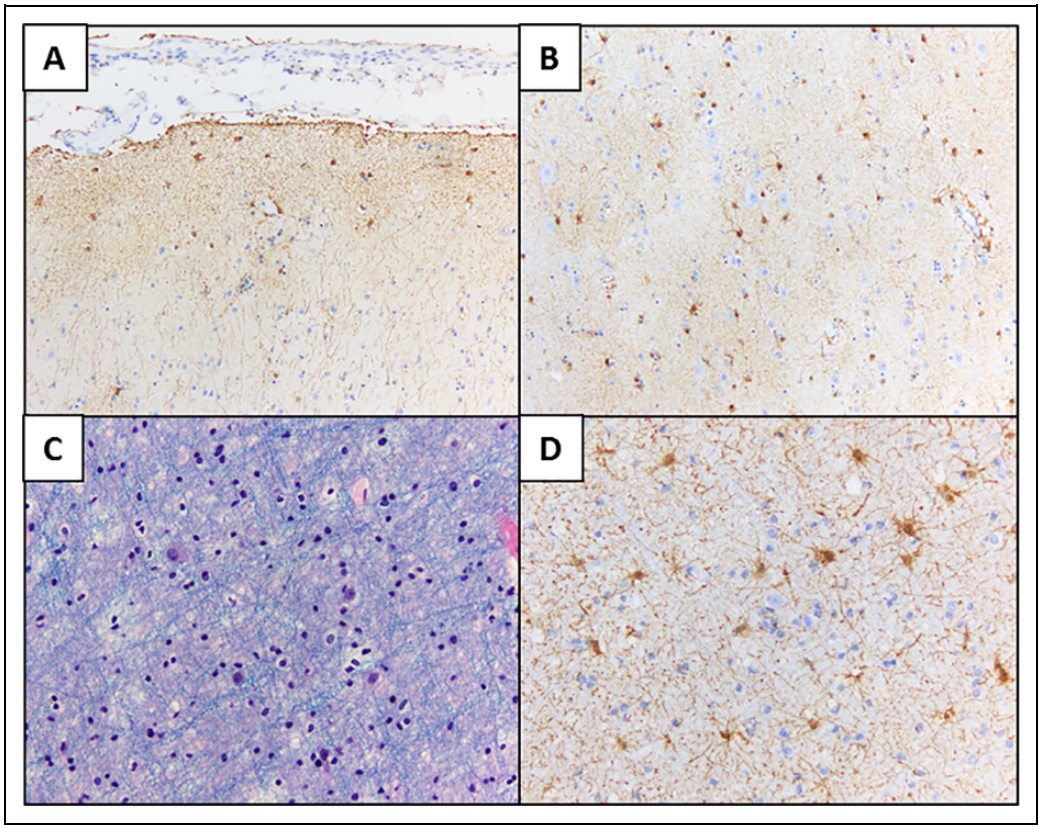


**Figure 1.** GFAP (glial fibrillary acidic protein) immunohistochemistry of fixed parietal cortex from the patient. (A) Subpial and layer I; (B) layers V/VI; (C) LFB/H&E (D) subcortical white matter with displaced neurons (arrow heads). (A, B: original magnification ×200; C, D: original magnification ×400.)

ALDH5A1=aldehyde dehydrogenase 5A1=SSADH). Although both open-label and placebo-controlled blinded trials have been completed (www.clinicaltrials.gov/NCT02019667[3]), current therapeutics remain symptomatic, and predominantly targeting either behavior (obsessive compulsive disorder, attention-deficit hyperactivity disorder [ADHD]) or seizure control. The sole therapeutic targeting the GABA pathway is the antiepileptic vigabatrin (irreversible inhibitor of GABA-transaminase; figure 1 in Kirby et al[1]), yet its clinical efficacy has been mixed and its risk of retinal toxicity complicates long-term consideration.[4] The patient was first reported by Haan et al[5] and again recently by Kirby et al[1] postmortem. A brief summary of clinical details is presented in Materials and Methods. Characterization of the pathophysiology of SSADHD has been significantly enhanced with the development of a knockout mouse model in 2001.[6] Electrophysiological studies in this model identified a pattern of seizure evolution, starting with absence seizures and progressing to generalized tonic-clonic convulsions with eventual status epilepticus.[7-9] Metabolic characterization has identified significant amino acid disturbances, imbalance of neurotransmitters and neurotransmitter precursors (elevated GABA, the GABA-analogue gamma-hydroxybutyrate, aspartate; depleted glutamine[1]) that are accompanied by significant downregulation of GABA receptors.[10,11] Many metabolic abnormalities detected in the murine model have been confirmed in patient physiological fluids.[12,13] Vogel and coworkers[14] verified disruption of GABAergic/glutamatergic receptor gene expression in brain of the mouse model that was responsive to mTOR inhibition. Until now, however, central nervous system tissue from an SSADHD patient has not been available for confirmatory studies.

In the first paper in this series,[1] amino acids, acylcarnitines, guanidino- species (guanidinoacetic acid, creatine, creatinine) and GABA-related intermediates were quantified in human postmortem frontal and parietal lobes, pons, cerebellum, hippocampus, cerebral cortex, liver, and kidney. Amino acid analyses revealed significant elevation of aspartic acid and depletion of glutamine in the patient, disruption of short-chain fatty acid metabolism, and elevation of GABA-related metabolites (GABA, γ-hydroxybutyrate, succinic semialdehyde, 4-guanidinobutyrate, homocarnosine; figure 1 in Kirby et al[1]), accompanied by disturbances of the creatine biosynthetic pathway. In the current report, we extend these metabolic studies to examine histopathology, lipid content, and gene expression in the same tissues. The following hypotheses were evaluated: (1) patient cortex/hippocampus would reveal astrogliosis[6,15]; (2) ethanolamine glycerophospholipid content in patient brain sections would be decreased[16,17]; and (3) downregulation of GABAergic/glutamatergic receptor subunits would be observed).[1,7,8,9,14]

## Materials and Methods

### Informed Consent, Patient, and Control Tissue Procurement

The studies herein reported were approved by the Human Research Ethics Committee of the Royal Melbourne Hospital, Parkville, Victoria, Australia, as well as the Institutional Review Board of the National Disease Research Interchange, Philadelphia, PA, USA. The family of the patient consented both to autopsy and procurement of tissues for experimental investigations and consented to publication of the data.

The patient was first reported in 1985.[5] In childhood, the patient's clinical course was typical of SSADHD, featuring global developmental delays, hypotonia, ataxia, and an absence of formalized speech. Throughout adolescence and into adulthood (second to third decades of life), his clinical history included epilepsy, autism, and an underactive thyroid and a diagnosis of Hashimoto thyroiditis. He was treated with risperidone. During respite care at the age of 37 years, he expired overnight with a postmortem diagnosis of SUDEP. Because his diagnosis was known, follow-up studies of electroencephalography (EEG), magnetic resonance imaging (MRI), or computed tomography (CT) were not undertaken. Following a period of almost 72 hours (cadaver stored at 4 °C), autopsy and tissue harvest was undertaken. Description of patient tissues and procurement of control tissues has been reported.[1] Samples of the peripheral nervous system, striatal muscle, spinal cord, and peripheral nerves were not obtained at autopsy. More in-depth evaluation of the brainstem, including the nucleus/fasciculus solitarius and the nucleus ambiguus, were also not biopsied at autopsy. It is not possible to make completely confident comparisons when contrasting analytical studies in tissues that were approximately 72 hours of age at harvest (patient) as compared to tissues harvested within 24 hours (controls[1]). Because only a single measure was afforded for the patient in each brain region, statistical analysis was not possible apart from gene expression studies. These caveats are considered in data interpretation. Although the patient was an adult, SSADHD is considered a pediatric neurotransmitter disorder and most patients are diagnosed in early childhood.

### Neuropathology

Histologic examination of human postmortem brain tissue was performed as described previously.[18] Briefly, formalin-fixed paraffin-embedded tissue was sectioned and stained with hematoxylin & eosin and Luxol fast blue prior to examination. GFAP polyclonal antibody was obtained from Dako (Agilent Pathology Solutions, Santa Clara, CA). Immunohistochemistry staining was performed on a Dako Autostainer Link48 (Agilent Pathology Solutions), according to standard operating procedure.

### Tissue Lipid Extraction

Lipids in the brain samples were extracted using a Tenbroeck homogenizer and a single-phase system of *n*-hexane–2-propanol (HIP, 3:2 v/v, 4 mL).[19] The extract was removed and the homogenizer rinsed with HIP (4 mL), which was added to the original extract. The extract was subjected to centrifugation at 2500×*g* for 15 minutes at –10 °C to pellet the protein. The supernatant containing the lipid extract was removed and dried under a stream of nitrogen, then dissolved and subjected to ultrafiltration using a 0.2-µm Nylon filter to remove residual proteins. The sample was dried under a stream of nitrogen and dissolved in *n*-hexane–2-propanol–water (56.7:37.5:5.5 v/v/v) prior to separation by high-performance liquid chromatography.

### High-Performance Liquid Chromatography

Phospholipids were separated by high-performance liquid chromatography and individual phospholipid classes were collected to quantify mass. This method separates all major phospholipid classes including ethanolamine glycerophospholipids (EtnGpl), lysophosphatidylethanolamine (lysoPtdEtn), phosphatidylinositol (PtdIns), phosphatidylserine (PtdSer), choline glycerophospholipids (ChoGpl), sphingomyelin (CerPCho), and lysophosphatidylcholine (lysoPtdCho) with baseline resolution. Phospholipid elution was monitored by UV absorbance at 205 nm. Authentic standards purchased from Avanti Polar Lipids (Alabaster, AL) were used to confirm elution order and retention time of phospholipid classes.

The high-performance liquid chromatography system used consisted of a Beckman Coulter System Gold 127 Solvent Module (Fullerton, CA), Beckman Coulter System Gold 166 Detector, Supelco Zorbax silica column (Bellefonte, PA) (25 cm × 4.6 mm, 5 µm), and Kipp & Zonen BD-41 recorder. Solvents were high-performance liquid chromatography grade purchased from EMD Millipore-Sigma (St Louis, MO). Solvent A was *n*-hexane–2-propanol (3:2 v/v) and solvent B was *n*-hexane–2-propanol–water (56.7:37.8:5.5 v/v/v). Initial proportions were 70% A–30% B with a flow rate of 1.5 mL/min, increasing proportion of solvent B in a stepwise manner until it reached 100% at 100 minutes, yielding baseline resolution of all phospholipids analyzed.

### Plasmalogen Mass

Following separation of phospholipid classes by high-performance liquid chromatography, the EtnGpl and ChoGpl fractions were quantitatively divided. One-half of each fraction was dried under a stream of nitrogen and subjected to mild acid hydrolysis of the plasmalogen vinyl ether linkage,[20] yielding an acid-stable fraction containing PakEtn (1-*O*-alkyl, 2-acyl glyceroethanolamine)/PtdEtn and PakCho (1-*O*-alkyl, 2-acyl glycerocholine/PtdCho), and an acid-labile fraction containing lysoPtdEtn (1-lyso, 2-acyl glycerolethanolamine) and lysoPtdCho (1-lyso, 2-acyl glycerocholine), which originated from the acid-labile PlsEtn and PlsCho, respectively. The mild acid hydrolysis removes the vinyl ether–linked fatty alcohol on the *sn*-1 position of the plasmalogen, resulting in a lyso position at the *sn*-1 position. Therefore, the plasmalogens were separated as lysophospholipids using the same solvent system described above. Initial solvent proportions were 45% solvent B and 55% solvent A at a flow rate of 1.8 mL/min, increasing to 100% B over 20 minutes. Plasmalogen mass was calculated using the EtnGpl and ChoGpl masses collected in the major phospholipid class separation and the proportion of lysophospholipid: phospholipid collected in the plasmalogen separation.

### Phospholipid Mass

Phospholipid and plasmalogen masses were quantified by measuring lipid phosphorus.[21] Briefly, lipid fractions were collected and dried overnight in an oven set at 85 °C. Phospholipids were digested with 0.5 mL water and 0.65 mL concentrated perchloric acid at 185 °C for 1 hour and allowed to cool. Then, 0.5 mL ascorbic acid in water (10% w/v), 0.5 mL ammonium molybdate in water (2.5% w/v), and 3.3 mL water were added to each tube, vortexed well, and placed in a heating block at 100 °C for 5 minutes. Inorganic phosphorus mass was

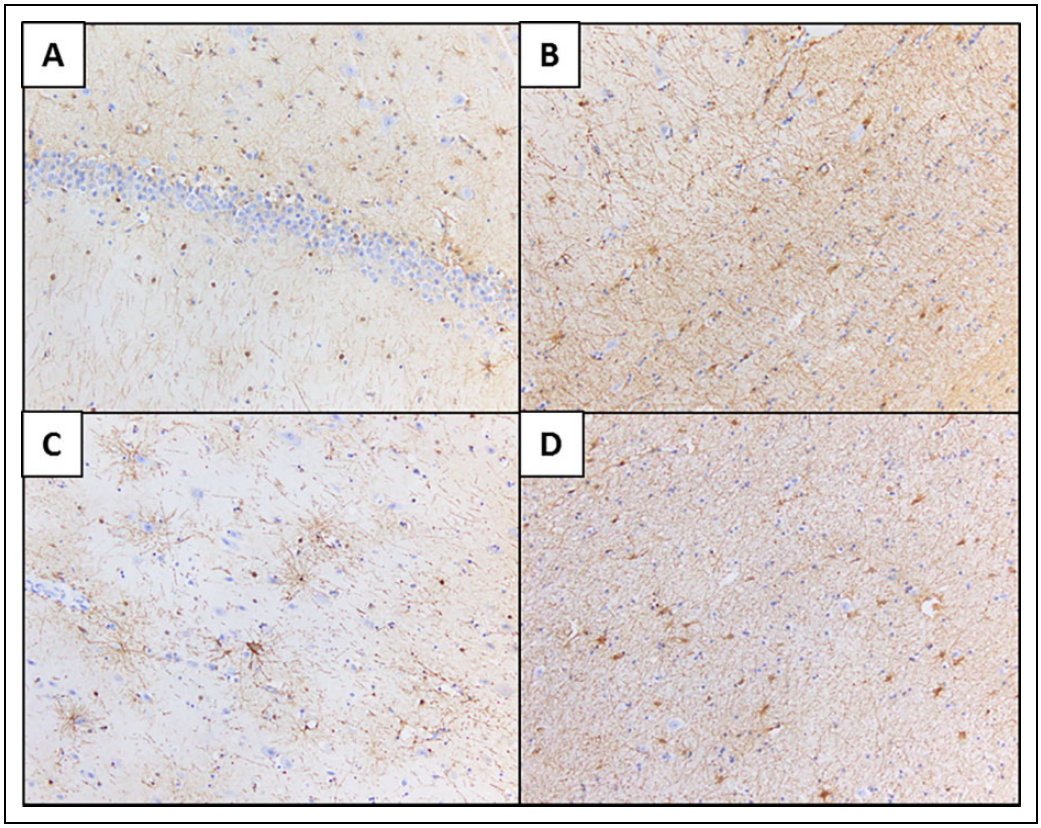


**Figure 2.** GFAP (glial fibrillary acidic protein) immunohistochemistry of fixed hippocampal section from the patient. (A) Dentate gyrus; (B) polymorphous layer; (C) entorhinal cortex; (D) entorhinal subcortical white matter (original magnification ×200).

quantified by absorbance at 797 nm and compared to a standard curve of known nmol of phosphorus.

### *Gene Expression Analyses*

Total RNA was isolated from cerebellum, frontal cortex, and parietal cortex using the miRNeasy Mini Kit (Qiagen) according to manufacturer's protocol. RNA was not extracted from the other regions because of lack of tissue. Quality of RNA was assessed by nanodrop and fragment analyzer (Agilent). RNA was quantified by Qubit Assay (Invitrogen). cDNA was synthesized using the RT2 First Strand Kit (Qiagen), and the Human GABA & Glutamate $RT^2$ profiler array (Qiagen) was selected for gene expression analysis. $RT^2$ profiler arrays were run on a CFX 384 (BioRad) instrument. Data analysis was performed using the GeneGlobe (Qiagen) platform, which calculated relative expression to the geometric mean of the housekeeping genes GAPDH (glyceraldehyde 3-phosphate) and ACTB (β-actin) using the delta delta CT method (essentially "log-fold change"). For data analysis, the fold regulation threshold was 2.0, and the *P* value threshold was .05.

## Results

Histology in fixed cortex and hippocampus of the patient revealed mild to moderate reactive astrogliosis, as assessed by GFAP immunohistochemistry, particularly in white matter areas of the brain (Figures 1 and 2). In the parietal cortex, mild reactive astrogliosis was present in the subpial region as well as cortical layers I, V, and VI (Figure 1A, B). Additionally, increased numbers of white matter neurons and moderate reactive astrogliosis was observed in the underlying cortical white matter (Figure 1C, D). Similar patterns of reactive gliosis were observed in the hippocampus, with mild gliosis in the dentate gyrus and entorhinal cortex and moderate gliosis in the hippocampal polymorphous layer and entorhinal subcortical white matter (Figure 2).

We observed several putative changes, defined as 2 standard deviations from the mean of the control group, in phospholipid mass between the control group and patient. In the cortex, the patient had a marked 61% increase in total phospholipid mass (nanomoles phospholipid/gram wet weight) from the mean of the control values (Table 2A). Conversely, total phospholipid mass in the hippocampus was decreased 51% in the patient as compared to the controls (Table 5A). In the cerebellum, frontal lobe, pons, and parietal lobe, total phospholipid masses were not considered different between the patient and control group. Hence, the total phospholipid levels were increased only in the patient's cortical section and decreased in the patient's hippocampal section.

Because the changes in total phospholipid mass may not reflect changes in every phospholipid class, the masses of individual phospholipid classes were analyzed. As expected from the total phospholipid data, the patient's cortex had increased levels of each major phospholipid class as compared to control

**Table 1.** Cerebellum (A) Phospholipid and (B) Plasmalogen Mass in SSADH-Deficient Patient and Control Group.[a]

| (A) Phospholipid Mass | | | | | | |
|---|---|---|---|---|---|---|
| | nmol/g ww | | | mol % | | |
| | Patient | Mean (control) | SD | Patient | Mean (control) | SD |
| EtnGpl | 11 965 | 12 228 | 4572 | 38.1 | 37.8 | 1.4 |
| PtdIns | 1173 | 1445 | 137 | 3.7 | 4.8 | 1.4 |
| PtdSer | 3103 | 3228 | 1625 | 9.9 | 9.7 | 1.7 |
| ChoGpl | 11 947 | 12 100 | 3660 | 38.1 | 38.1 | 1.8 |
| CerPCho | 3208 | 3123 | 1130 | 10.2 | 9.7 | 0.2* |
| Total | 31 397 | 32 125 | 11 103 | | | |
| | n = 1 | n = 3 | | | | |
| (B) Plasmalogen Mass | | | | | | |
| EtnGpl | 5052 | 5999 | 1693 | 42.2 | 50.3 | 6.5 |
| PlsEtn | 6913 | 6229 | 3063 | 57.8 | 49.7 | 6.5 |
| ChoGpl | 10 464 | 10 853 | 3079 | 87.6 | 90.0 | 1.8 |
| PlsCho | 1483 | 1247 | 595 | 12.4 | 10.0 | 1.8 |
| | n = 1 | n = 3 | | | | |

[a]Mass values are expressed as nmol phosphorus/gram wet weight tissue and represent mean ± SD of control and patient values. Molar composition values are expressed as mol % of total phosphorus. n = 2-4.
*Indicates significance between patient and control group, 2 SD from control mean.

**Table 2.** Cortex (A) Phospholipid and (B) Plasmalogen Mass in SSADH-Deficient Patient and Control Group.[a]

| (A) Phospholipid and Mass | | | | | | |
|---|---|---|---|---|---|---|
| | nmol/g ww | | | mol % | | |
| | Patient | Mean (control) | SD | Patient | Mean (control) | SD |
| EtnGpl | 28 099 | 17 735 | 1395* | 40.7 | 42 | 3.3 |
| PtdIns | 2393 | 1607 | 178* | 3.5 | 3.75 | 0.3 |
| PtdSer | 9308 | 4973 | 547* | 13.5 | 11.6 | 0.5* |
| ChoGpl | 21 319 | 14 612 | 1619* | 30.9 | 34.1 | 2.3 |
| CerPCho | 7934 | 3838 | 355* | 11.5 | 9.0 | 0.7* |
| Total | 69 053 | 42 765 | 2905* | | | |
| | n = 1 | n = 4 | | | | |
| (B) Plasmalogen Mass | | | | | | |
| EtnGpl | 11 536 | 7311 | 598* | 41.1 | 41.6 | 6.4 |
| PlsEtn | 16 563 | 10 424 | 1861* | 58.9 | 58.4 | 6.4 |
| ChoGpl | 19 621 | 13 233 | 1479* | 92.0 | 90.6 | 0.9 |
| PlsCho | 1698 | 1379 | 195 | 8.0 | 9.4 | 0.9 |
| | n = 1 | n = 4 | | | | |

[a]Mass values are expressed as nmol phosphorus/gram wet weight tissue and represent mean ± SD of control and patient values. Molar composition values are expressed as mol % of total phosphorus. n = 2-4.
*Indicates significance between patient and control group, 2 SD from control mean.

values. In the patient's cortex, the EtnGpl mass was increased 58%, the PtdSer mass was increased 49%, the PtdIns mass was increased 87%, the ChoGpl mass was increased 46%, and CerP-Cho mass was increased 107% as compared to controls (Table 2A). In contrast, the mass of each major phospholipid class was significantly decreased in the patient's hippocampal sample as compared to the control group, reflective of the large decrease in total phospholipid mass (Table 5A). In the patient's hippocampus, the EtnGpl mass was decreased 52%, the PtdIns mass was decreased 47%, the PtdSer mass was decreased 65%, the ChoGpl mass was decreased 39%, and the CerPCho mass was decreased 63% as compared to control values (Table 5A). Interestingly, in the patient's frontal lobe, only the patient's PtdSer level was decreased 63% compared to the control group (Table 3A). In the patient's pons, the EtnGpl mass was increased 44% and the ChoGpl mass was increased 42% as compared to the control values (Table 4A). Although we observed large changes in the hippocampus and cortex that were nonspecific

**Table 3.** Frontal Lobe (A) Phospholipid and (B) Plasmalogen Mass in SSADH-Deficient Patient and Control Group.[a]

| (A) Phospholipid Mass | nmol/g ww | | | mol % | | |
|---|---|---|---|---|---|---|
| | Patient | Mean (control) | SD | Patient | Mean (control) | SD |
| EtnGpl | 12 519 | 16 153 | 2886 | 38.2 | 39 | 1.6 |
| PtdIns | 1549 | 1840 | 243 | 4.7 | 4.5 | 0.6 |
| PtdSer | 1792 | 4818 | 1390* | 5.5 | 11.5 | 2.1* |
| ChoGpl | 14 339 | 14 474 | 2338 | 43.7 | 35.2 | 3.9* |
| CerPCho | 2614 | 4036 | 1032 | 8.0 | 9.7 | 1.7 |
| Total | 32 812 | 41 321 | 6911 | | | |
| | n = 1 | n = 4 | | | | |
| (B) Plasmalogen Mass | | | | | | |
| EtnGpl | 7027 | 6512 | 1295 | 56.1 | 40.6 | 5.8* |
| PlsEtn | 5492 | 9641 | 2191 | 43.9 | 59.4 | 5.8* |
| ChoGpl | 12 924 | 12 912 | 2236 | 90.1 | 89.1 | 1.1 |
| PlsCho | 1415 | 1562 | 147 | 9.9 | 10.9 | 1.1 |
| | n = 1 | n = 4 | | | | |

[a]Mass values are expressed as nmol phosphorus/gram wet weight tissue and represent mean ± SD of control and patient values. Molar composition values are expressed as mol % of total phosphorus. n = 2-4.
*Indicates significance between patient and control group, 2 SD from control mean.

in terms of phospholipid class, the frontal lobe and pons showed class-specific changes in phospholipid mass.

Plasmalogens are a subclass of phospholipids that contain a vinyl ether linkage in the sn-1 position. Because plasmalogens are enriched in arachidonic acid, they are considered a putative intracellular signaling molecule with a role in lipid-mediated signal transduction,[22,23] we also analyzed plasmalogen mass in each group. In the cortex, the mass of the acid-stable fractions of EtnGpl and ChoGpl were increased 58% and 48%, respectively, while the PlsEtn mass was increased 58% in the patient as compared to the control group (Table 2B). In the pons, the acid-stable fraction of EtnGpl was increased 30%, whereas the PlsEtn mass was increased 50% and the PlsCho mass was increased 39% as compared to control values (Table 4B). In the hippocampus, the patient PlsEtn mass was decreased 70% and the acid-stable ChoGpl fraction was decreased 38% compared to the control group (Table 5B). Therefore, the plasmalogen mass was reflective of the change in major glycerophospholipid mass except for the hippocampus, where the PlsEtn mass was significantly decreased and the acid-stable fraction of EtnGpl was unchanged. No major abnormalities in plasmalogen mass were detected in cerebellum or parietal lobe (Tables 1B, 6B).

Phospholipid molar composition was also determined, and values are expressed as a molar percent of the total phospholipid mass. Molar composition is useful to assess changes in metabolism of certain lipid classes, and indeed, several interesting alterations were noted. In the cerebellum, the proportion of CerPCho was slightly increased 6% from control values (Table 1A). Although there was a marked increase in phospholipid mass noted in the cortex (Table 2A), proportional changes were limited to PtdSer (16% increase) and CerPCho (28% increase) compared with control values. Interestingly, in the frontal lobe, the proportion of PtdSer was decreased 53%, as expected from the decrease in its mass, but the proportion of ChoGpl was increased 24% as compared to controls (Table 3A). Further, the acid-stable fraction of EtnGpl was increased 38%, whereas the proportion of PlsEtn was decreased 26% compared to the control group (Table 3B).

The pons showed compositional changes in several phospholipid classes (Table 4A). The proportion of EtnGpl and ChoGpl were increased 10% and 11%, respectively compared to control patient values. Slight, but potentially important, increases in PlsEtn (4%) and the acid-stable fraction (10%) accompanied the increase in EtnGpl (Table 4B). In contrast, the proportions of PtdSer and CerPCho were decreased 24% and 16%, respectively. In the hippocampus, the proportion of ChoGpl was increased 25%, while the proportion of CerPCho was decreased 22% as compared to controls (Table 5A). Additionally, the proportion of PlsEtn was markedly decreased 36% (Table 5B). Lastly, in the parietal lobe, the proportion of EtnGpl was slightly increased 6% from controls (Table 6A). As opposed to phospholipid mass, in which the observed changes were largely nonspecific, the molar composition analysis revealed several proportional changes in PtdSer, CerPCho, ChoGpl, and PlsEtn.

Gene expression are shown in Tables 7 and 8. Negative values indicate downregulation, positive values upregulation. A total of 84 genes were assessed in total RNA from cerebellum, frontal and parietal lobes of the patient. Of 15 $GABA_A$ receptor subunits analyzed, the patient revealed dysregulation of 14 in at least 1 tissue (predominantly downregulation). Downregulation of $\alpha 4$ and $\alpha 5$ subunits in cerebellum were accompanied by upregulation in other tissues (Table 7). The most significant levels of downregulation levels were observed

**Table 4.** Pons (A) Phospholipid and (B) Plasmalogen Mass in SSADH-Deficient Patient and Control Group.[a]

| (A) Phospholipid Mass | | | | | | |
|---|---|---|---|---|---|---|
| | nmol/g ww | | | mol % | | |
| | Patient | Mean (control) | SD (control) | Patient | Mean (control) | SD (control) |
| EtnGpl | 26 536 | 18 428 | 2549* | 44.8 | 41.0 | 1.0* |
| PtdIns | 1031 | 978 | 153 | 1.7 | 2.2 | 0.7 |
| PtdSer | 6911 | 6991 | 1572 | 11.7 | 15.4 | 1.0* |
| ChoGpl | 18 820 | 13 290 | 2543* | 31.8 | 29.4 | 0.8 |
| CerPCho | 5933 | 5396 | 852 | 10.0 | 12.0 | 0.1* |
| Total | 59 231 | 45 083 | 7361 | | | |
| | n = 1 | n = 2 | | | | |
| (B) Plasmalogen Mass | | | | | | |
| EtnGpl | 7044 | 5407 | 590* | 26.5 | 29.4 | 0.9* |
| PlsEtn | 19 492 | 13 021 | 1959* | 73.5 | 70.6 | 0.9* |
| ChoGpl | 16 526 | 11 640 | 2705 | 87.8 | 87.2 | 3.7 |
| PlsCho | 2293 | 1650 | 163* | 12.2 | 12.8 | 3.7 |
| | n = 1 | n = 2 | | | | |

[a]Mass values are expressed as nmol phosphorus/gram wet weight tissue and represent mean ± SD of control and patient values. Molar composition values are expressed as mol % of total phosphorus. n = 2-4.
*Indicates significance between patient and control group, 2 SD from control mean.

**Table 5.** Hippocampus (A) Phospholipid and (B) Plasmalogen Mass in SSADH-Deficient Patient and Control Group.[a]

| (A) Phospholipid Mass | | | | | | |
|---|---|---|---|---|---|---|
| | nmol/g ww | | | mol % | | |
| | Patient | Mean (control) | SD | Patient | Mean (control) | SD |
| EtnGpl | 11 667 | 24 408 | 2882* | 40.1 | 41.0 | 2.5 |
| PtdIns | 826 | 1562 | 389* | 2.8 | 2.6 | 0.3 |
| PtdSer | 3031 | 8751 | 2405* | 10.4 | 14.45 | 2.2 |
| ChoGpl | 10 824 | 17 730 | 1810* | 37.2 | 29.8 | 1.6* |
| CerPCho | 2761 | 7376 | 1630* | 9.5 | 12.2 | 1.1* |
| Total | 29 110 | 59 827 | 8523* | | | |
| | n = 1 | n = 4 | | | | |
| (B) Plasmalogen Mass | | | | | | |
| EtnGpl | 6933 | 8815 | 1331 | 59.4 | 36.9 | 10.2 |
| PlsEtn | 4734 | 15 593 | 3986* | 40.6 | 63.1 | 10.2* |
| ChoGpl | 9728 | 15 751 | 2256* | 89.9 | 88.5 | 4.3 |
| PlsCho | 1096 | 1979 | 530 | 10.1 | 11.5 | 4.3 |
| | n = 1 | n = 4 | | | | |

[a]Mass values are expressed as nmol phosphorus/gram wet weight tissue and represent mean ± SD of control and patient values. Molar composition values are expressed as mol % of total phosphorus. n = 2-4.
*Indicates significance between patient and control group, 2 SD from control mean.

for ε, θ, ρ1, and ρ2 subunits (7.7-9.9-fold). Unexpectedly, we found little effect on the $GABA_B$ receptor, and minimal dysregulation in the expression of either ionotropic or metabolomic glutamate receptors, apart from consistent downregulation of the metabotropic glutamate receptor 6 (Table 7). For genes encoding solute carriers, downregulation of the $Na^+$-dependent inorganic phosphate cotransporter 6 and the neurotransmitter transporter for GABA, member 13 (3.4-7.3-fold) were consistent findings. For 38 additional genes associated with GABAergic/glutamatergic activity, 15 showed dysregulation in at least 1 tissue of the patient (Table 8), including consistent downregulation of interleukin 1β (up to 9.9-fold) and upregulation of synuclein α (up to 6.5-fold).

## Discussion

The availability of these postmortem tissues represented a unique opportunity for metabolic and molecular investigations

**Table 6.** Parietal Lobe (A) Phospholipid and (B) Plasmalogen Mass in SSADH-Deficient Patient and Control Group. [a]

| (A) Phospholipid Mass | | | | | | |
|---|---|---|---|---|---|---|
| | nmol/g ww | | | mol % | | |
| | Patient | Mean (control) | SD | Patient | Mean (control) | SD |
| EtnGpl | 18 209 | 16 292 | 4543 | 41.7 | 39.5 | 0.4* |
| PtdIns | 1093 | 1209 | 245 | 2.5 | 3.0 | 0.3 |
| PtdSer | 5404 | 5430 | 2205 | 12.4 | 12.8 | 2.2 |
| ChoGpl | 14 766 | 14 015 | 2866 | 33.8 | 34.6 | 3.4 |
| CerPCho | 4214 | 4297 | 1624 | 9.6 | 10.2 | 1.4 |
| Total | 43 685 | 41 243 | 11 383 | | | |
| | n = 1 | n = 3 | | | | |
| (B) Plasmalogen Mass | | | | | | |
| EtnGpl | 5960 | 7314 | 732 | 32.7 | 46.8 | 10.2 |
| PlsEtn | 12 249 | 8977 | 3812 | 67.3 | 53.2 | 10.2 |
| ChoGpl | 13 303 | 12 727 | 2934 | 90.1 | 90.4 | 2.8 |
| PlsCho | 1463 | 1288 | 100 | 9.9 | 9.6 | 2.8 |
| | n = 1 | n = 3 | | | | |

[a]Mass values are expressed as nmol phosphorus/gram wet weight tissue and represent mean ± SD of control and patient values. Molar composition values are expressed as mol % of total phosphorus. n = 2-4.

*Indicates significance between patient and control group, 2 SD from control mean.

with the potential to further delineate pathomechanisms in SSADHD. There are obvious limitations to the interpretation of our findings, including the delay from time of death to tissue harvest, the inability to accurately match control tissues for age and medications, the limited number of control specimens, and the fact that the patient was receiving risperidone at time of death.[1] Fortunately, risperidone does not appear to specifically target GABAergic/glutamatergic receptors, or solute carrier systems.[24]

For the first time, we have shown the presence of astrogliosis in selected brain regions of a patient with SSADHD, confirming earlier studies in the brain of null mice.[6,15] Reactive astrogliosis was present in the patient's cortex, subcortical white matter, and hippocampus. Although gliosis in and of itself is not specific for any specific pathologic entity, it is a useful marker for subtle or early pathologic changes and can also reflect chronic injury to a particular brain region. It is particularly useful to identify pathologic insult in cases such as epilepsy that do not display overt loss of neurons/myelin or have a robust inflammatory response.

Previous studies on lipid alterations in SSADH deficiency have demonstrated alterations consistent with myelin dysfunction in a gene-ablated mouse model.[16,17] In the current study, we focused on phospholipids, one of the most abundant class of lipids in the myelin sheath,[25-27] and identified several putative differences with control values. The patient's cortical and hippocampal samples had marked changes in total phospholipid mass, which were unexpectedly increased in the cortical sample (61%) and decreased in the hippocampal sample (51%). This was reflected in the mass of each of the major phospholipid classes in these regions (Tables 2A and 5A). In the cortex, there were also significant increases in the acid-stable and plasmalogen fractions of ethanolamine glycerophospholipids (EtnGpl), as expected (Table 2B). However, the molar composition of the cortex revealed proportional increases in phosphatidylserine (PtdSer) and sphingomyelin (CerPCho) (Table 2A). Taken together, the increase in the proportion of PtdSer and CerPCho along with the increase in total phospholipids suggest that the patient's cortical sample was contaminated with myelin. Myelin contains a greater proportion of phospholipids per unit fresh weight by 40%,[27] and include greater proportions of PtdSer and CerPCho.[28,29] Further, these cortical data contradict prior studies in which myelin proteins are downregulated and PlsEtn is decreased in the cortices of SSADH-deficient mice).[16,17] Therefore, because the cortex shows a significant increase in the total phospholipid mass as well as proportions of CerPCho and PtdSer, this is suggestive of myelin contamination in the patient sample as compared to the control group, accounting for the unexpected increase in mass.

Consistent with previous studies on SSADH-deficient mice,[16,17] the remaining brain regions reveal several phospholipid changes that may be related to the observed decreases in myelin components observed in gene-ablated mice. Phospholipid proportions differ in white matter and gray matter, with decreased proportions of PtdIns and ChoGpl, and increased proportions of EtnGpl, PlsEtn, PtdSer, and CerPCho seen in white matter.[28,29] Interestingly, these same changes were observed in samples from the pons, hippocampus, and frontal lobe. The proportion of CerPCho was decreased in the pons and hippocampus (Tables 4A and 5A), whereas PtdSer was decreased in the pons and frontal lobe (Tables 4A and 3A). In the frontal lobe and hippocampus, the proportion of ChoGpl was significantly increased (Tables 3A and 5A) whereas the

**Table 7.** Dysregulation of GABAergic, Glutamatergic, and Solute Carrier Genes in Cerebellum and Frontal/Parietal Lobes of the Patient.[a]

| | Subunit | Cerebellum | Frontal lobe | Parietal lobe | Comment |
|---|---|---|---|---|---|
| $GABA_AR$ | α2 | −2.56 | | | |
| | α4 | −2.77 | | 2.32 | |
| | α5 | −4.19 | 2.12 | 2.63 | |
| | α6 | | | −2.34 | |
| | β1 | −4.84 | −2.26 | −4.46 | |
| | β3 | | | 2.49 | |
| | δ | | | −2.56 | |
| | ε | −3.95 | −4.71 | −7.71 | |
| | γ1 | −2.35 | | | |
| | γ2 | | | 2.0 | |
| | γ3 | −4.37 | | | |
| | θ | −3.08 | −3.35 | −8.81 | |
| | ρ1 | −2.73 | −3.18 | −9.86 | |
| | ρ2 | | −3.69 | −9.86 | |
| $GABA_BR$ | R2 | | | −2.3 | |
| Glu R | A1 | −2.92 | | | Ionotropic AMPA 1 |
| | A4 | | | −2.17 | Ionotropic AMPA 4 |
| | K5 | | | −3.31 | Ionotropic kainate 5 |
| | N1 | | | −2.22 | Ionotropic NMDA 1 |
| | 1 | | | −2.11 | Metabotropic 1 |
| | 5 | | | −2.82 | Metabotropic 5 |
| | 6 | −2.1 | −4.0 | −5.87 | Metabotropic 6 |
| | 8 | | | | Metabotropic 8 |
| SLC | 17A6 | −3.37 | −2.18 | −2.21 | $Na^+$-dependent $P_i$ cotransporter member 6 |
| | 17A8 | −2.62 | | | $Na^+$-dependent $P_i$ cotransporter member 8 |
| | 1A3 | −3.67 | 2.26 | | Glial high affinity glu transporter member 3 |
| | 1A6 | −2.18 | | | High affinity asp/glu transporter member 6 |
| | 6A13 | −2.89 | −2.02 | −7.3 | Neurotransmitter transporter, GABA, member 13 |
| | 7A11 | | 2.57 | | Anionic amino acid transporter, light chain, $xc^-$ system member 11 |

Abbreviations: AMPA, α-amino-3-hydroxy-5-methyl-4-isoxazolepropionic acid; asp, aspartate; cere, cerebellum; glu, glutamate; NMDA, N-methyl-D-aspartate; $P_i$, inorganic phosphate; R, receptor; SLC, solute carrier; $xc^-$, cystine-glutamate antiporter.

[a] All values shown significant at $P < .05$. Negative, downregulation; positive, upregulation. Of the 51 genes evaluated for expression levels, 29 revealed dysregulation in at least 1 tissue from the patient.

proportion of PlsEtn was decreased (Tables 3B and 5B). Although the patient group was n = 1, the pattern present in these brain regions suggests brainwide alterations in lipid metabolism that favor myelin derangement and support the conclusions from previous studies).[16,17]

We formulated our hypothesis of dysregulated GABAergic/glutamatergic receptor subunits based on earlier studies in the null mouse that revealed decreased expression both in hippocampal regions and in the whole brain.[7,8,14] Direct comparison of those data with current data in human are not possible, because here we have looked at specific human regions in an RNA-dependent approach. However, the prediction that GABAergic receptor systems would be downregulated generally held forth (Table 7), especially $GABA_A$ receptors. Conversely, glutamatergic receptors were considerably less impacted, except for the metabotropic glutamate receptor 6 (Table 7). As well, specific solute carrier genes were also impacted, especially the SLC17a6 (inorganic phosphate cotransporter, or vesicular glutamate transporter; VGLUT2) and SLC6a13 (GABA transporter 2; GAT-2). Whether both genes are downregulated due to GABA, or glutamate, or a combination of both is unknown, but there was no frank elevation of glutamate in brain regions of the patient.[1]

Gene expression results were notable in patient tissues that were not dysregulated (glutamic acid decarboxylase, GABA-transaminase, glutaminase [predominantly neuronally located] and glutamine-ammonia ligase [predominantly glial located][14]). The enzymes encoded by these genes are responsible for maintenance of the GABA-glutamine-glutamate cycle, which is disrupted in the brain of the null mouse but has not been studied in human SSADHD.[30] As well, all 4 genes were downregulated in the null mouse brain.[14] Further, $GABA_B$ receptor subunits (R1, R2) were not downregulated in the patient, which is at variance with our past animal work.[7,9] $GABA_B$ receptor subunit findings may also help to explain the lack of efficacy of the $GABA_B$ receptor antagonist SGS-742 which was recently administered in a double-blind, placebo-controlled study in SSADHD (Schreiber et al., unpublished).

We observed downregulations of specific purinergic/adenosine receptors as well as calcium channels and receptor-signaling proteins (phospholipase A2, C), but these changes were not ubiquitous across tissues and predominantly centered

**Table 8.** Dysregulation of Miscellaneous Genes Associated With GABAergic/Glutamatergic Signaling in Cerebellum and Frontal/Parietal Lobes of the Patient. [a]

| Gene | Cerebellum | Frontal lobe | Parietal lobe | Comment |
|---|---|---|---|---|
| IL1β | –3.78 | –2.93 | –9.86 | Interleukin 1, β |
| ITPR1 | –2.32 | | –2.4 | Inositol 1,4,5-triphosphate receptor, type 1 |
| P2RX7 | –2.81 | –2.03 | | Purinergic receptor P2X, ligand-gated ion channel, 7 |
| ADCY7 | | | –2.4 | Adenylate cyclase 7 |
| SHANK2 | | –2.08 | –2.97 | SH3 and multiple ankyrin repeat domains 2 |
| ADORA2A | | | –2.98 | Adenosine A2a receptor |
| CACNA1A | | | –2.21 | Calcium channel, voltage dependent, P/Q type, α1A subunit |
| CACNA1B | | | –3.02 | Calcium channel, voltage dependent, N type, α1A subunit |
| CLN3 | | | –2.17 | Ceroid lipofuscinosis, neuronal 3 |
| PLA2G6 | | | –2.35 | Phospholipase A2, group VI (cytosolic, $Ca^{+}$2-independent |
| PLCB1 | | | –2.11 | Phospholipase C, β1 (phosphoinositide specific) |
| MAPK1 | 6.54 | | | Mitogen-activated protein kinase 1 |
| SNCA | 5.08 | 4.88 | 6.52 | Synuclein, α (non A4 component of amyloid precursor) |
| AVP | –2.34 | | –2.95 | Arginine vasopressin |

[a]All values shown significant at $P < .05$. Negative, downregulation; positive, upregulation. Of the 38 genes evaluated for expression levels, 15 revealed dysregulation in at least 1 tissue from the patient. This group of genes contained 38 genes in total, for which the 15 shown in the table were dysregulated in at least 1 of the patient's tissues.

on parietal lobe (Table 8). Ren and Mody[31] demonstrated that exogenous GHB, which is highly elevated in patient brain,[1] induces phosphorylation/activation of MAPK1 via $GABA_B$ receptor function, and this is consistent with upregulation of MAPK1 in cerebellum (Table 8). Other genes of interest dysregulated in the patient included IL1β, synuclein α, and arginine vasopressin. Emmanouilidou and coworkers[32] demonstrated that GABA transmission regulates α-synuclein secretion in mouse striatum via ATP-dependent $K^+$ channels, consistent with the findings of upregulation for SNCA in the patient across regions. Moreover, earlier studies demonstrated that brain neutral lipid mass was increased, as was turnover of brain phospholipids, in α-synuclein gene-ablated mice.[25,33] This suggests that the upregulation observed for SNCA in patient brain (Table 8) may be associated with the alterations of lipid and plasmalogen classes we observed for the patient.

Downregulation of IL1β across all patient brain regions was interesting yet challenging to explain. Bianchi and colleagues[34] documented that administration of IL1β to mice significantly reduced hippocampal GABA. Supraphysiological GABA levels, as seen in SSADHD,[1] may conversely lead to downregulation of IL-1β, underscoring the interrelationships of GABA metabolism in the central modifications induced by IL-1β. Finally, arginine vasopressin was massively downregulated in previous gene expression studies on the null mouse brain,[14] but only slightly downregulated in our patient's tissues. The elevation of 4-guanidinobutyrate (a putative derivative of GABA and arginine[1,35]) in the brain regions of our patient may provide insight into this downregulation.[1]

In sum, the current results provide a broader understanding of the underlying pathophysiology of human SSADHD. To assist potential future postmortem studies, should they unfortunately occur, we are developing a protocol that will allow rapid and extensive collection of brain tissue, peripheral tissue biopsies, and physiological fluids to add to our biorepository of specimens that is a component of our ongoing natural history study of SSADHD.

## Author Note

Contributing Authors for the SSADH Deficiency Investigators Consortium (SDIC): Phillip L. Pearl[1], Jean-Baptiste Roullet[2], K. Michael Gibson[2], Christos Papadelis[3], Thomas Opladen[4], Alexander Rotenberg[1], Kiran Maski[1], Melissa Tsuboyama[1], Simon Warfield[5], Onur Afacan[5], Edward Yang[5], Carolyn Hoffman[6], Kathrin Jeltsch[4], Jeffrey Krischer[7], M. Ángeles García Cazorla[8], Erland Arning[9]

[1]Department of Neurology, Boston Children's Hospital, Harvard Medical School, Boston, MA, USA; [2]College of Pharmacy and Pharmaceutical Sciences, Department of Pharmacotherapy, Washington State University, Spokane, WA, USA; [3]Jane and John Justin Neuroscience Center, Cook Children's Health Care System; Department of Pediatrics, Texas Christian University and the University of North Texas Health Sciences Center, School of Medicine, Fort Worth, TX, USA; and the Laboratory of Children's Brain Dynamics, Division of Newborn Medicine, Boston Children's Hospital, Harvard Medical School, Boston, MA, USA; [4]Department of Child Neurology and Metabolic Disorders, University Children's Hospital, Heidelberg, Germany; [5]Department of Radiology, Boston Children's Hospital, Harvard Medical School, Boston, MA, USA; [6]SSADH Association; [7]Health Informatics Institute, Morsani College of Medicine, University of South Florida, Tampa, FL, USA; [8]Servicio de Neurologia and CIBERER, ISCIII, Hospital San Joan de Deu, Barcelona, Spain; [9]Institute of Metabolic Disease, Baylor Research Institute, Dallas, Texas, USA

## Acknowledgments

We gratefully acknowledge the family of the patient for agreeing to submission of autopsied tissues. We thank Dr Timothy Fazio and Ms Christine Fischer, Metabolic Disease Unit, Royal Melbourne Hospital, Victoria, Australia, for procurement, coordination, and shipment of tissues. We acknowledge the assistance of Dr William Rizzo in interpretation of the brain lipid results.

## Author Contributions

DCW and RL contributed equally to the study. All authors contributed to the study conception, design, and execution. Data collection and analysis were performed by DCW, TK, RL, JTA, MPA, and EJM. Data reduction, statistical analyses, and the first draft of the manuscript was performed by DCW, TK, JBR, and KMG. Final oversight of data analyses, interpretation, and editing of the manuscript were performed by EJM, JBR, and KMG. All authors commented on previous versions of the manuscript. The SSADH Deficiency consortium provided critical SSADH deficiency research background to the study and support in subject recruitment. All authors read and approved the final manuscript.

## Declaration of Conflicting Interests

The authors declared no potential conflicts of interest with respect to the research, authorship, and/or publication of this article.

## Funding

The authors disclosed receipt of the following financial support for the research, authorship, and/or publication of this article: This study was generously supported by the SSADH Association (www.ssadh.net), R01HD091142 from the National Institute of Child Health, National Institutes of Health (KMG), and R13NS116963 from the National Institute of Neurological Disorders and Stroke, National Institutes of Health (J-BR).

## ORCID iD

Dana C. Walters https://orcid.org/0000-0002-4761-7505
K. Michael Gibson https://orcid.org/0000-0003-4465-1318

## References

1. Kirby T, Walters DC, Brown M, et al. Post-mortem tissue analyses in a patient with succinic semialdehyde dehydrogenase deficiency (SSADHD). I. Metabolomic outcomes. *Metab Brain Dis*. 2020;35:601-614.
2. Malaspina P, Roullet JB, Pearl PL, Ainslie GR, Vogel KR, Gibson KM. Succinic semialdehyde dehydrogenase deficiency (SSADHD): pathophysiological complexity and multifactorial trait associations in a rare monogenic disorder of GABA metabolism. *Neurochem Int*. 2016;99:72-84.
3. Schreiber JM, Pearl PL, Dustin I, et al. Biomarkers in a taurine trial for succinic semialdehyde dehydrogenase deficiency. *JIMD Rep*. 2016;30:81-87.
4. Police A, Shankar VK, Murthy SN. Role of taurine transporter in the retinal uptake of vigabatrin. *AAPS PharmSciTech*. 2020;21:196.
5. Haan EA, Brown GK, Mitchell D, Danks DM. Succinic semialdehyde dehydrogenase deficiency—a further case. *J Inherit Metab Dis*. 1985;8:99.
6. Hogema BM, Gupta M, Senephansiri H, et al. Pharmacologic rescue of lethal seizures in mice deficient in succinate semialdehyde dehydrogenase. *Nat Genet*. 2001;29:212-216.
7. Wu Y, Buzzi A, Frantseva M, et al. Status epilepticus in mice deficient for succinate semialdehyde dehydrogenase: GABAA receptor-mediated mechanisms. *Ann Neurol*. 2006;59:42-52.
8. Buzzi A, Wu Y, Frantseva MV, et al. Succinic semialdehyde dehydrogenase deficiency: GABAB receptor-mediated function. *Brain Res*. 2006;1090:15-22.
9. Cortez MA, Wu Y, Gibson KM, Snead OC 3rd. Absence seizures in succinic semialdehyde dehydrogenase deficient mice: a model of juvenile absence epilepsy. *Pharmacol Biochem Behav*. 2004;79:547-553.
10. Gupta M, Polinsky M, Senephansiri H, et al. Seizure evolution and amino acid imbalances in murine succinate semialdehyde dehydrogenase (SSADH) deficiency. *Neurobiol Dis*. 2004;16:556-562.
11. Gibson KM, Schor DS, Gupta M, et al. Focal neurometabolic alterations in mice deficient for succinate semialdehyde dehydrogenase. *J Neurochem*. 2002;81:71-79.
12. Jansen EE, Vogel KR, Salomons GS, Pearl PL, Roullet JB, Gibson KM. Correlation of blood biomarkers with age informs pathomechanisms in succinic semialdehyde dehydrogenase deficiency (SSADHD), a disorder of GABA metabolism. *J Inherit Metab Dis*. 2016;39:795-800.
13. Vogel KR, Ainslie GR, Walters DC. Succinic semialdehyde dehydrogenase deficiency, a disorder of GABA metabolism: an update on pharmacological and enzyme-replacement therapeutic strategies. *J Inherit Metab Dis*. 2018;41:699-708.
14. Vogel KR, Ainslie GR, Gibson KM. mTOR inhibitors rescue premature lethality and attenuate dysregulation of GABAergic/glutamatergic transcription in murine succinate semialdehyde dehydrogenase deficiency (SSADHD), a disorder of GABA metabolism. *J Inherit Metab Dis*. 2016;39:877-886.
15. Brown MN, Gibson KM, Schmidt MA, et al. Cellular and molecular outcomes of glutamine supplementation in the brain of SSADH-deficient mice. *JIMD Rep*. 2020;56:58-69.
16. Donarum EA, Stephan DA, Larkin K, et al. Expression profiling reveals multiple myelin alterations in murine succinate semialdehyde dehydrogenase deficiency. *J Inherit Metab Dis*. 2006;29:143-156.
17. Barcelo-Coblijn G, Murphy EJ, Mills K, et al. Lipid abnormalities in succinate semialdehyde dehydrogenase (Aldh5a1$^{-/-}$) deficient mouse brain provide additional evidence for myelin alterations. *Biochim Biophys Acta*. 2007;1772:556-562.
18. Ahrendsen JT, Anderson KR, Anderson MP. Lymphocytic ganglionitis leading to megacolon in lymphocyte-rich glioblastoma. *J Neuroimmunol*. 2019;337:577075.
19. Hara A, Radin NS. Lipid extraction of tissues with a low-toxicity solvent. *Anal Biochem*. 1978;90:420-426.
20. Murphy EJ, Stephens R, Jurkowitz-Alexander M, Horrocks LA. Acidic hydrolysis of plasmalogens followed by high-performance liquid chromatography. *Lipids*. 1993;28:565-568.
21. Rouser G, Siakotos AN, Fleischer S. Quantitative analysis of phospholipids by thin-layer chromatography and phosphorus analysis of spots. *Lipids*. 1969;1:85-86.
22. Farooqui AA, Yang HC, Horrocks LA. Plasmalogens, phospholipases A2 and signal transduction. *Brain Res Rev*. 1995;21:152-161.
23. Rosenberger TA, Oki J, Purdon AD, Rapoport SI, Murphy EJ. Rapid synthesis and turnover of brain microsomal ether phospholipids in the adult rat. *J Lipid Res*. 2002;43:59-68.
24. Gao L, Feng S, Liu ZY, Wang JQ, Qi KK, Wang K. A computational network analysis based on targets of antipsychotic agents. *Schizophr Res*. 2018;193:154-160.

25. Barcelo-Coblijn G, Golovko MY, Weinhofer I, Berger J, Murphy EJ. Brain neutral lipids mass is increased in α-synuclein gene-ablated mice. *J Neurochem*. 2007;101:132-141.
26. Sun GY, Horrocks LA. The fatty acid and aldehyde composition of the major phospholipids of mouse brain. *Lipids*. 1968;3:79-83.
27. Morell P, Raine C. *Myelin*, ed. Morell P. Boston, MA: Springer US; 1984.
28. Horrocks LA. Composition of myelin from peripheral and central nervous systems of the squirrel monkey. *J Lipid Res*. 1967;8: 569-576.
29. Sun GY, Sun AY. Phospholipids and acyl groups of synaptosomal and myelin membranes isolated from the cerebral cortex of squirrel monkey (Saimiri sciureus). *Biochim Biophys Acta*. 1972;280: 306-315.
30. Chowdhury GM, Gupta M, Gibson KM, Patel AB, Behar KL. Altered cerebral glucose and acetate metabolism in succinic semialdehyde dehydrogenase-deficient mice: evidence for glial dysfunction and reduced glutamate/glutamine cycling. *J Neurochem*. 2007;103:2077-2091.
31. Ren X, Mody I. Gamma-hydroxybutyrate reduces mitogen-activated protein kinase phosphorylation via GABA B receptor activation in mouse frontal cortex and hippocampus. *J Biol Chem*. 2003;278:42006-42011.
32. Emmanouilidou E, Minakaki G, Keramioti MV, et al. GABA transmission via ATP-dependent $K^+$ channels regulates α-synuclein secretion in mouse striatum. *Brain*. 2016;139: 871-890.
33. Golovko MY, Rosenberger TA, Feddersen S, Færgeman NJ, Murphy EJ. α-Synuclein gene ablation increases docosahexaenoic acid incorporation and turnover in brain phospholipids. *J Neurochem*. 2007;101:201-211.
34. Bianchi M, Ferrario P, Zonta N, Panerai AE. Effects of interleukin-1 beta and interleukin-2 on amino acids levels in mouse cortex and hippocampus. *Neuroreport*. 1995;6:1689-1692.
35. Jansen EE, Verhoeven NM, Jakobs C, et al. Increased guanidino species in murine and human succinate semialdehyde dehydrogenase (SSADH) deficiency. *Biochim Biophys Acta*. 2006;1762: 494-498.